

A 122 GHz SiGe Active Subharmonic Mixer

A. Müller, M. Thiel, H. Irion, and H.-O. Ruoff

Robert Bosch GmbH, Corporate Sector Research and Advance Engineering,
Dept. CR/ARE, Robert-Bosch-Platz 1, 70839 Gerlingen-Schillerhöhe, Germany,
+49 711 811 38458, andreas.mueller12@de.bosch.com

Abstract—A 122 GHz subharmonic mixer for a radar-based sensor has been realized. It is fabricated in SiGe:C-HBT technology with a transit frequency of about 200 GHz. The conversion gain of the mixer is 23 dB at a LO-frequency of 60 GHz with +3 dBm of power and a RF-input of 122.5 GHz. The measured SSB noise figure at 122.5 GHz is 12 dB.

I. INTRODUCTION

There is a growing demand for measuring physical parameters like distance and speed contactlessly. Radar sensors present an attractive solution to obtain the relevant parameters directly or indirectly from the reflected RF-signal. The fact that the operation of radar sensors is almost independent from surrounding conditions, e.g. rain or strong sunlight, makes them attractive for many applications. As the availability of installation space is more and more reduced, it is inevitable to shrink the overall size of the sensor as well.

Increasing the operation frequency is a suitable strategy to decrease the size of a sensor without making restrictions to the antenna performance. Therefore, frequencies beyond 100 GHz are very attractive for the design of small radar sensors.

As the field of application extends from automotive functions to industrial- and security-technology, it is important to obtain a very low-cost sensor. Silicon based technology allows high volume production and the increase of integration density.

SiGe technology offers a great potential to come up to the demands concerning performance, integration and low-cost. We use the 0.25 μm SGC25 process from IHP providing HBTs with a transit frequency f_T of about 200 GHz [1].

II. CIRCUIT TOPOLOGY

As millimeter-wave signals are frequently generated using push-push oscillators [2] it is convenient to strive for a mixer that uses the oscillator's fundamental frequency for down-conversion. The objective is to realize an active subharmonic mixer that is pumped by the fundamental signal of the push-push oscillator. A resistive mixer solution is not desired as not complying with the requirements concerning conversion characteristics.

A. Subharmonic mixer core

With integrated circuits, the Gilbert-cell is one of the most popular balanced direct mixer designs. An active subharmonic mixer based on the Gilbert-topology is another basic building block for the realization of an integrated radar front-end at millimeter-wave frequencies.

Doubling the LO-switching-cycle is the basis for even harmonic operation. In this work a design as described in [3] is used. The basic Gilbert mixer design is extended by a further line of LO-switching transistors yielding in a stacked

Gilbert-cell topology. Figure 1 illustrates the schematic of the circuit and the principle of doubling the LO-switching-cycle.

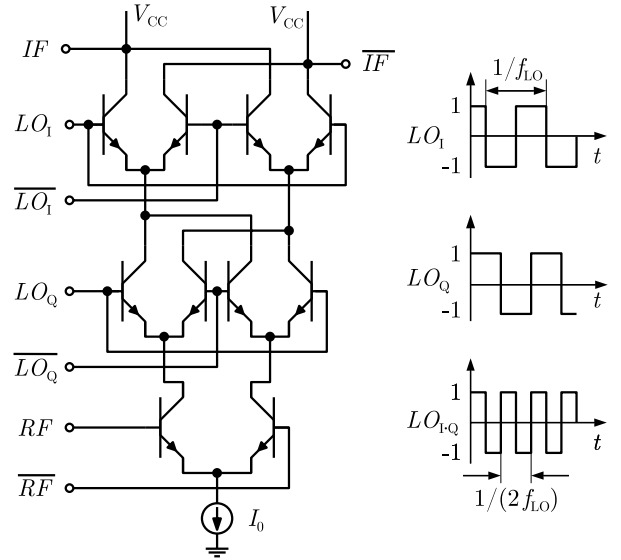


Fig. 1. Schematic and LO-switching-cycles of the subharmonic mixer.

The upper transistor pairs are supplied with the $0^\circ/180^\circ$ phasing of the LO-signal and denoted in-phase component (LO_1 and $\overline{LO_1}$). The so-called quadrature component, with a phasing of $90^\circ/270^\circ$ (LO_Q and $\overline{LO_Q}$), is applied to the second row of transistor pairs. The single switching cycles of both LO transistor pairs are shown on the right hand side of figure 1. The quadrature signal that is applied to the stacked LO stages yields the product LO_{1-Q} which is twice the LO-switching-cycle, as depicted in the last row of the graph. Concerning the RF transistor pair no modification has to be made.

B. Polyphase structure

Polyphase filters represent a very common solution for providing the required LO-phases. For lower microwave frequencies they are realized using lumped elements. As this might be difficult at 60 GHz we decided to obtain the phases in a different way.

A combination of branch-line couplers is used for the supply of the mixer core with the necessary phases. The network consists of three hybrid couplers that are connected as depicted in figure 2.

The first coupler and the two subsequent lines (ϕ and $\phi + 90^\circ$) generate the differential in-phase LO-signal

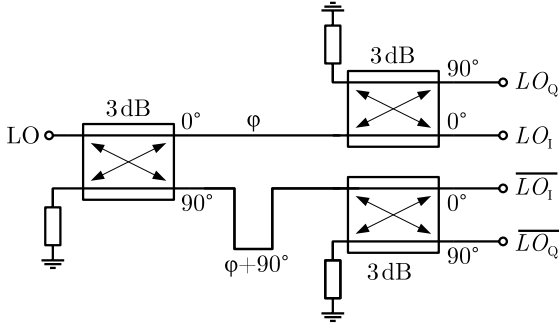


Fig. 2. Simplified schematic of the hybrid phase network.

(0°/180°). The two succeeding couplers complete the signal with the differential quadrature component (90°/270°). The major disadvantage of this distributed network is its size. On a thin film substrate with a thickness of 4.16 μm and a relative dielectric constant of $\epsilon_r = 3.9$, a 3dB-hybrid-coupler using $\lambda/4$ lines measures about 0.4 mm². Hence, the overall size of the proposed phase network would be greater than 1 mm². Reducing the size of the structure is of course indispensable. For this work reduced-size couplers with capacitive load are used. The design is carried out as described in [4].

By shortening the coupler lines to $\lambda/8$ the coupler size decreases to 0.1 mm². Besides the use of shunt capacitances the design requires higher line impedances by the factor of $\sqrt{2}$. Figure 3 shows the schematic coupler design.

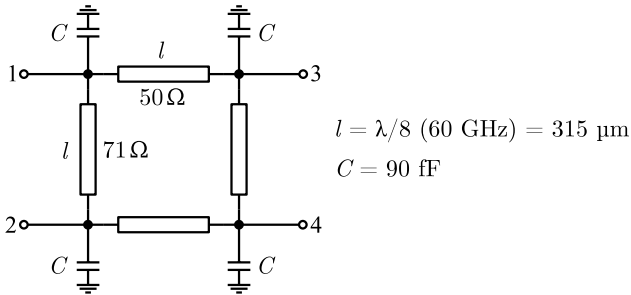


Fig. 3. Capacitively loaded hybrid coupler for 60GHz.

The design was optimized to reduce the amplitude inequalities to a minimum. Realizing a layout with meander shaped lines is an additional way to reduce area consumption.

For the characterization of the subharmonic mixer we add a buffer stage to the differential IF-output of the core. It consists of a differential amplifier and an emitter follower, which also transforms the differential signal to a single-ended output. The usage of this circuit is a good compromise to increase gain with moderate noise influence as the buffer operates far below the transit frequency.

The overall power consumption of the mixer is about 150mW from a voltage supply at 6.6V. However, the mixer core itself draws only a current of 3mA, whereas the buffer stage consumes the major part with 20mA. An optimization is not yet performed.

III. MEASUREMENT RESULTS

The measurements are carried out on separated chips. The local-oscillator signal is generated with a multiplier that quadruples a 15GHz input signal. The maximum output power at 60GHz is +4dBm on-chip. With an attenuator it is possible to reduce LO-power to -34dBm. For the RF-signal we used the VNWA extension from OML in combination with an attenuator. This combination provides variable power between -43dBm and -13dBm on-chip. The IF output is directly fed to the spectrum analyzer.

A. Conversion characteristics

First, the conversion gain in dependency of the applied local-oscillator power is investigated. A LO-frequency of 60GHz is applied. With a RF-signal at 122.5GHz ($P_{RF} = -34$ dBm) the mixing product is 2.5GHz. The result is given in figure 4.

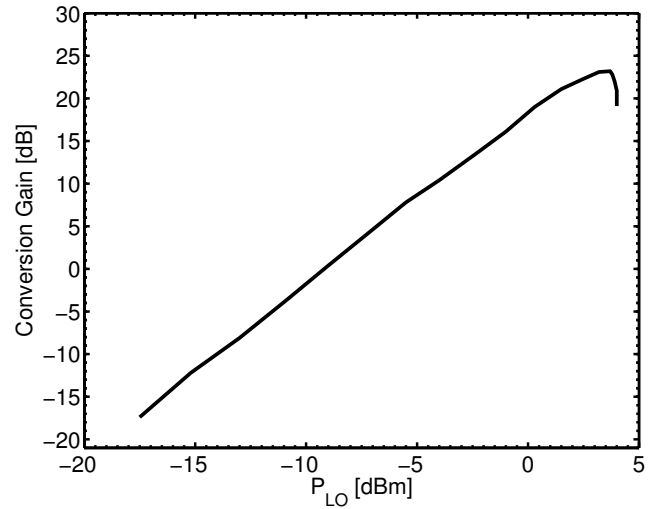


Fig. 4. Conversion gain vs. applied local-oscillator power at an intermediate frequency of 2.5GHz.

The mixer shows a linear gain characteristic for P_{LO} between -17dBm and +3dBm. The maximum conversion gain is 23dB at +3dBm LO-power. Although the local-oscillator output power is limited to +4dBm it can be observed that the gain decreases above the maximum. The mixer core itself was simulated with a gain of 4dB for $P_{LO} = +3$ dBm.

Another interesting point is the dependence on the variation of the local-oscillator frequency. A LO signal between 60.05GHz and 61GHz with -3dBm power is applied. With a fixed RF-signal at 122.5GHz and $P_{RF} = -34$ dBm the intermediate frequency is between 500MHz and 2.4GHz. The result is shown in figure 5.

The graph indicates a certain frequency dependence. The curve is somewhat flat from 60.5GHz up to 61GHz and depicts a maximum conversion gain of about 17dB. Below 60.5GHz a decreasing gain is stated.

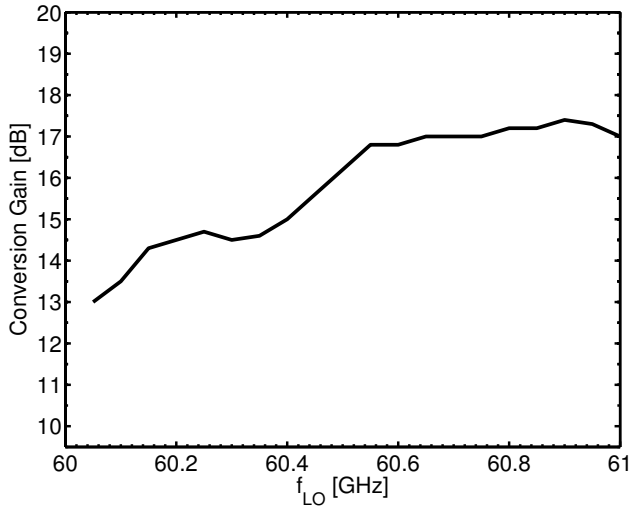


Fig. 5. Conversion gain vs. applied local-oscillator frequency. The local-oscillator power is set to -3 dBm.

In addition to the intermediate-frequency at 2.5 GHz ($f_{LO} = 60$ GHz and $f_{RF} = 122.5$ GHz) the output signal of the mixer contains a 2^{nd} harmonic at 5 GHz as well. This is the conversion product of four times the LO- and twice the RF-signal. The RF-power is set again to -34 dBm. The power-levels at the IF-port obtained for both harmonics versus the applied local-oscillator power are pointed out in figure 6.

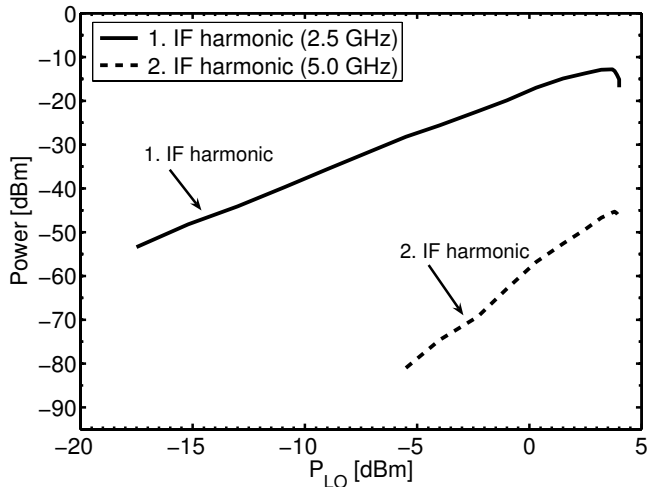


Fig. 6. Signal level of the 1^{st} and 2^{nd} harmonic of the intermediate frequency vs. applied local-oscillator power at a RF power of -34 dBm.

The curves show that in the range of -5 dBm to $+5$ dBm the signal level of the 2^{nd} harmonic is much lower than the level of the 1^{st} harmonic. The 2^{nd} harmonic is suppressed with more than 30 dB.

B. Noise performance

Besides the conversion characterization noise measurements are accomplished. As a noise source in the 122 GHz region is not available it was not possible to apply the very common hot/cold method. But since the gain of the device G_{DUT} is known and a low-noise behavior is not expected, the direct noise measurement method is deployed.

The output power at the device's IF-port is measured with a termination at the RF-port. The local-oscillator signal still feeds the device. A succeeding low-noise amplifier (gain G_1 and noise figure NF_1) boosts the IF-signal level. The measurement setup is illustrated in figure 7.

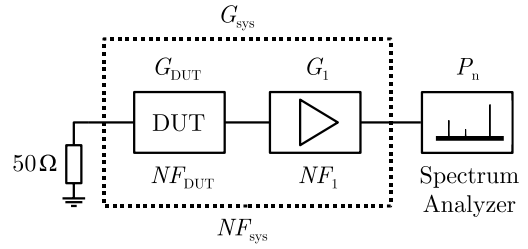


Fig. 7. Setup for the direct noise measurement method.

The thermal noise at the RF-input is calculated to:

$$10 \log \left(\frac{k_B T_0 \Delta f}{1 \text{ mW}} \right) = -174 \text{ dBm/Hz}, \quad (1)$$

where k_B is Boltzmann's constant and T_0 equals 290 K. The bandwidth taken into account is denoted Δf and is set to 1 Hz in equation 1. The noise figure of the system NF_{sys} is determined by the noise level P_n detected by the spectrum analyzer using

$$NF_{sys} = P_n + 174 \text{ dBm/Hz} - G_{sys}. \quad (2)$$

The measurements were carried out with a local-oscillator signal at 60 GHz and $+3$ dBm of power. The noise level is measured with a span of 1 kHz and a resolution bandwidth of 1 Hz. The noise level P_n of the measurement is illustrated in figure 8. The average level is approximately -91 dBm. The conversion gain of 23 dB together with the low-noise amplifier providing a gain of 48 dB leads to a system noise figure NF_{sys} of 12 dB.

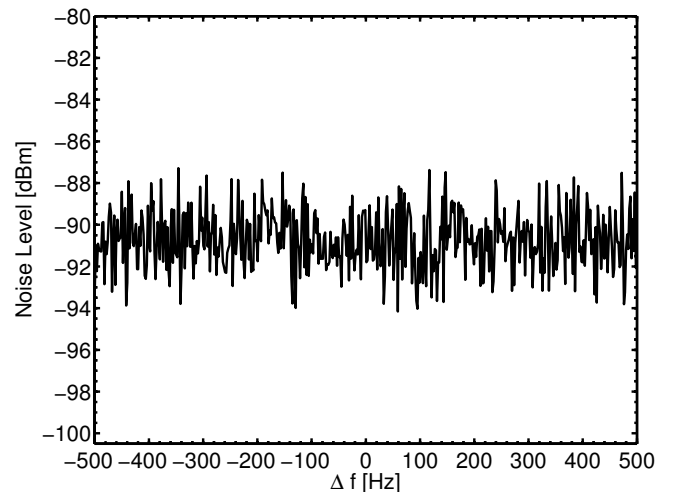


Fig. 8. Noise level at the IF-port at a center frequency of 2.5 GHz with 1 kHz span and a resolution bandwidth of 1 Hz.

By applying Friis' formula, one can calculate the resulting noise figure NF_{DUT} of the mixer. As the low-noise amplifier provides a noise figure of only 1.3 dB and the mixer has a very high gain, the the system noise figure NF_{sys} is almost

equal to the mixer's noise figure NF_{DUT} .

A chip photo is shown in figure 9. The chip-size without all pads is 0.75 mm^2 .

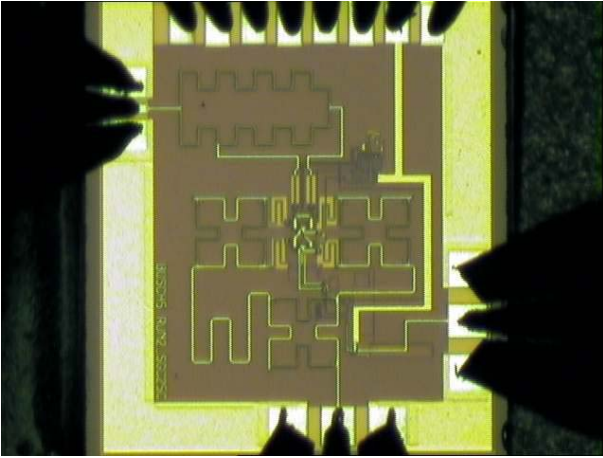


Fig. 9. Chip photo with contacted probes.

The RF-signal is fed by a probe head with $50\text{ }\mu\text{m}$ pitch from the left side. As balun a meander shaped rat-race coupler was used. On the right side the IF signal is tapped with a $150\text{ }\mu\text{m}$ probe. The chip is supplied with the local-oscillator signal from the bottom using a probe head with $150\text{ }\mu\text{m}$ pitch. The photo shows the arrangement of the compact hybrid-couplers for the phase generation. The DC-probe is connected from top providing the 6.6 V supply voltage.

IV. CONCLUSION

A subharmonic mixer for ISM applications at 122 GHz in SiGe:C technology is presented. The use of a stacked Gilbert cell leads to even harmonics with respect to the local-oscillator frequency at 60 GHz . The generation of the four necessary phases is done with a cascade of three capacitively loaded branch-line couplers. The mixer shows a maximum conversion gain of 23 dB . Higher order mixing terms were identified at 5 GHz only. The signal level is more than 30 dB lower in comparison with the 1st order IF. Using the direct noise measurement method the noise figure of the mixer is determined to 12 dB . With that, a key component for the integration of a mm-wave radar front-end is realized successfully, demonstrating the potential of current state-of-the-art SiGe processes.

REFERENCES

- [1] W. Winkler, B. Heinemann, D. Knoll, "Application of SiGe:C BiCMOS to Wireless and Radar", *12th Gallium Arsenide and other Compound Semiconductors Application Symposium*, vol. 1, pp. 259–262, 11–12 October 2004.
- [2] M. Steinhauer, H. Irion, M. Schott, M. Thiel, H.-O. Ruoff, W. Heinrich, "SiGe-Based Circuits for Sensor Applications beyond 100 GHz ", *IEEE MTT-S International Microwave Symposium Digest*, vol. 1, pp. 223–226, 6–11 June 2004.
- [3] R. Svitek and S. Raman, "A SiGe Active Sub-Harmonic Front-End for $5\text{--}6\text{ GHz}$ Direct Conversion Receiver Applications", *IEEE Radio Frequency Integrated Circuits Symposium*, pp. 675–678, 8–10 June 2003.
- [4] T. Hirota, A. Minakawa, M. Muraguchi, "Reduced-Size Branch-Line and Rat-Race Hybrids for Uniplanar MMIC's", *IEEE Transactions on Microwave Theory and Techniques*, vol. 38, no. 3, pp. 270–275, March 1990.